


 Cite this: *RSC Adv.*, 2019, 9, 27279

Induction of cryptic metabolites of the endophytic fungus *Trichocladium* sp. through OSMAC and co-cultivation†

 Nam Michael Tran-Cong,^a Attila Mándi,^b Tibor Kurtán,^b Werner E. G. Müller,^c Rainer Kalscheuer,^a Wenhan Lin,^d Zhen Liu^{*a} and Peter Proksch^{*a}

The endophytic fungus *Trichocladium* sp. isolated from roots of *Houttuynia cordata* was cultured on solid rice medium, yielding a new amidepsine derivative (**1**) and a new reduced spiro azaphilone derivative (**3**) together with eight known compounds (**4**–**11**). Co-cultivation of *Trichocladium* sp. with *Bacillus subtilis* resulted in induction of a further new compound (**2**) and a 10-fold increase of **11** compared to the axenic fungal culture. Moreover, when the fungus was cultivated on peas instead of rice, a new sesquiterpene derivative (**13**) and two known compounds (**12** and **14**) were obtained. Addition of 2% tryptophan to rice medium led to the isolation of a new bismacrolactone (**15**). The structures of the new compounds were elucidated by HRESIMS, 1D and 2D NMR as well as by comparison with the literature. A combination of TDDFT-ECD, TDDFT-SOR, DFT-VCD and DFT-NMR calculations were applied to determine the absolute and relative configurations of **13** and **15**. Compounds **7**, **11** and **15** exhibited strong cytotoxicity against the L5178Y mouse lymphoma cell line with IC₅₀ values of 0.3, 0.5 and 0.2 μM, respectively.

 Received 16th July 2019
Accepted 20th August 2019

DOI: 10.1039/c9ra05469c

rsc.li/rsc-advances

Introduction

Paclitaxel, a well-known and widely used anti-cancer compound, was first isolated from the bark of *Taxus brevifolia* by Wani *et al.* in 1971.¹ Later in 1993, Stierle *et al.* discovered that the endophytic fungus *Taxomyces andreanae* from the yew tree is able to produce taxol and other taxane derivatives.² This sparked detailed investigations of natural products from endophytes which confirmed these organisms as a promising source of new bioactive compounds.³ In continuation of our ongoing investigations on bioactive metabolites from fungi,^{4–6} an endophytic fungus *Trichocladium* sp. was isolated from roots of the plant *Houttuynia cordata* known in Vietnam as “fish mint”. Prior to renaming as *Trichocladium*, *Trichocladium* species have been listed in the literature under the genus *Humicola*.⁷ Fungi of the genus *Trichocladium* have been reported

to produce several bioactive secondary metabolites including inhibitors of serine proteases of the coagulation pathway, asterriquinones CT1, CT3 and CT4,⁸ a cytotoxic phenolic tetralone, humicolone,⁹ and inhibitors of human diacylglycerol acyltransferases (DGAT), amidepsines A–K.¹⁰

In this study, fermentation of *Trichocladium* sp. on solid rice medium yielded ten natural products (**1**, **3**–**11**) including two new compounds (**1** and **3**). Co-cultivation of *Trichocladium* sp. with *Bacillus subtilis* led to the production of a new compound (**2**) and a 10-fold increase of **11**. In addition, when the fungus was cultivated on peas instead of rice, a new sesquiterpene derivative (**13**) and two known compounds (**12** and **14**) that were not detected when the fungus was grown on rice medium were obtained. Compound **14** is a tryptophan derivative, inspiring us to add 2% tryptophan to rice medium in order to stimulate production of tryptophan derived compounds. Feeding of tryptophan led to the isolation of the new compound **15**, which represents a macrolide linked to an anthranilic acid moiety. The latter moiety is likely to be derived from feeding of tryptophan (Fig. 1).

Results and discussion

Compound **1** was obtained as pale yellow powder. Its molecular formula was determined as C₂₉H₂₇NO₁₃ by HREIMS, indicating seventeen degrees of unsaturation. The NMR data of **1** (Table 1) were similar to those of amidepsine J previously isolated from *Humicola* sp. FO-2942.¹⁰ Six aromatic protons at δ_H

^aInstitute of Pharmaceutical Biology and Biotechnology, Heinrich Heine University Düsseldorf, Universitätsstrasse 1, 40225 Düsseldorf, Germany. E-mail: zhenfeizi0@sina.com; proksch@uni-duesseldorf.de

^bDepartment of Organic Chemistry, University of Debrecen, P. O. Box 400, H-4002 Debrecen, Hungary

^cInstitute of Physiological Chemistry, Universitätsmedizin der Johannes Gutenberg-Universität Mainz, 55128 Mainz, Germany

^dState Key Laboratory of Natural and Biomimetic Drugs, Peking University, Beijing 100191, China

† Electronic supplementary information (ESI) available: MS, 1D and 2D NMR spectra of compounds **1**–**3**, **13** and **15** as well as the results of Marfey's reaction and computational calculations. See DOI: 10.1039/c9ra05469c



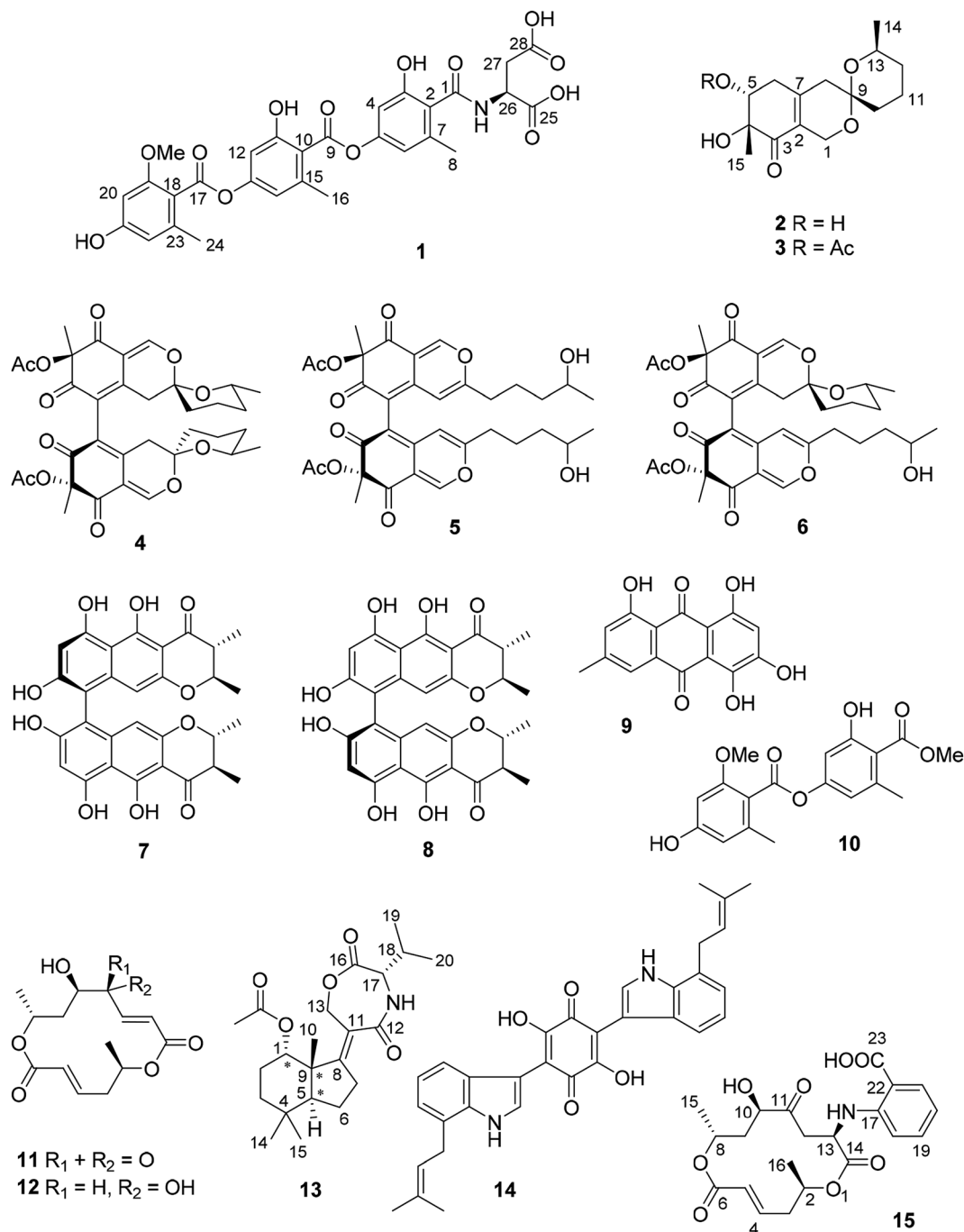


Fig. 1 Structures of isolated compounds from *Trichocladium* sp.

6.66 (H-12), 6.63 (H-14), 6.57 (H-4), 6.54 (H-6), 6.37 (H-20), and 6.31 (H-22) as well as three aromatic methyl groups at δ_{H} 2.37 (Me-16), 2.28 (Me-24), and 2.24 (Me-8) were observed. However, the NMR spectra of **1** showed signals of only one methoxy group at δ_{C} 55.8 and δ_{H} 3.79, instead of two methoxy groups as found for amidepsine J. The position of this methoxy group at C-19 was evident from the ROESY correlations between the protons of this methoxy group and H-20, and between H-20/21-OH (δ_{H} 9.96), 21-OH/H-22, H-22/Me-24. In addition, signals of a valine moiety were replaced by signals of an aspartic acid moiety (from C-25 to C-28) in **1**. The COSY correlations between 26-NH/H-26/

H-27ab and the HMBC correlations from 26-NH to C-1 together with the ROESY correlation between 26-NH and Me-8 indicated the linkage between the aspartic acid moiety and C-1 through an amide bond. The absolute configuration of the aspartic acid moiety was determined after acid hydrolysis of **1** followed by Marfey's method which indicated that the aspartic acid moiety was present in the L-form. Thus, the structure of compound **1** was elucidated as shown, representing a new amidepsine derivative, for which a trivial name amidepsine L is proposed.

The molecular formula of **2** was determined as C₁₅H₂₂O₅ based on the HRESIMS data. The NMR data of **2** (Table 2) were



Table 1 ^1H and ^{13}C NMR data of compound 1^a

Position	δ_{C} , type ^b	δ_{H} (J in Hz)
1	166.4, C	
2	123.2, C	
3	155.1, C	
4	106.5, CH	6.57, d (2.1)
5	150.6, C	
6	113.4, CH	6.54, d (2.1)
7	137.7, C	
8	18.9, CH ₃	2.24, s
9	165.8, C	
10	118.6, C	
11	156.1, C	
12	107.0, CH	6.66, d (2.0)
13	152.1, C	
14	114.1, CH	6.63, d (2.0)
15	137.8, C	
16	19.2, CH ₃	2.37, s
17	165.7, C	
18	112.8, C	
19	158.5, C	
20	97.0, CH	6.37, d (2.0)
21	160.1, C	
22	109.1, CH	6.31, d (2.0)
23	138.0, C	
24	19.4, CH ₃	2.28, s
25	172.6, C	
26	48.8, CH	4.69, dt (7.6, 6.6)
27	36.2, CH ₂	2.78, dd (16.4, 6.6) 2.61, dd (16.4, 6.6)
28	171.8, C	
11-OH		10.44, s
19-OMe	55.8, CH ₃	3.79, s
21-OH		9.96, s
26-NH		8.47, d (7.6)

^a Measured in DMSO-*d*₆ (^1H at 300 MHz and ^{13}C at 75 MHz). ^b Data were extracted from the HSQC and HMBC spectra.

very similar to those of pestafolide A.¹¹ However, the smaller coupling constants between H-5 and H-6ab (both 3.5 Hz) in 2 compared to those in pestafolide A (10.0 and 5.8 Hz) suggested that the orientation of H-5 was different in 2. This was further supported by the ROESY correlations between H-5 (δ_{H} 3.98)/Me-15 (δ_{H} 1.30), Me-15/H-6a (δ_{H} 2.70), and H-6a/H-5, indicating that these protons were on the same face of the cyclohexenone ring. The remaining substructure and stereochemistry of 2 were identical to those of pestafolide A as concluded after detailed analysis of the 2D NMR spectra of 2. Thus, compound 2 was identified as 5-*epi*-pestafolide A.

Comparison of the ^1H and ^{13}C NMR data between 2 and 3 (Table 2) revealed the appearance of an additional acetoxy group (δ_{C} 170.5 and 21.1, δ_{H} 2.01) in 2, which was also evident from the molecular formula of 3 (C₁₇H₂₄O₆) being 42 amu larger than that of 2. The downfield-shifted H-5 signal (δ_{H} 5.29, dd, J = 3.6, 2.3 Hz) in 3 compared to that in 2 (δ_{H} 3.98, t, J = 3.5 Hz) suggested the location of this additional acetoxy group at C-5, which was confirmed by the HMBC correlation from H-5 to the carbonyl carbon of the acetoxy group. The coupling constants of H-5 were similar in 2 and 3, indicating the same stereochemistry at C-5 for 2 and 3. In conclusion, compound 3

was elucidated as 5-*O*-acetyl-*epi*-pestafolide A. Storage of 2 in EtOAc over one week did not yield 3 indicating that 3 is a true natural product and not an artifact arising from 2 during workup of the extract.

The remaining known compounds isolated from rice medium were identified as cochliodones A (4), E (5) and H (6),^{12,13} chateochromin A (7),¹⁴ ustilaginoindin D (8),¹⁵ 5-hydroxymodin (9),¹⁶ methyl 2-*O*-methyllecanorate (10),¹⁷ and colletoketol (11).^{18–20}

In an OSMAC approach, the medium was changed from rice to peas. Investigation of the fungal culture on pea medium led to the isolation of colletodiol (12)²⁰ and asteriquinone CT4 (14)⁸ as well as of a new compound (13).

Compound 13 was isolated as white amorphous powder. On the basis of the HRESIMS data, the molecular formula of 13 was established as C₂₂H₃₃NO₅ with seven degrees of unsaturation. The ^1H NMR spectrum (Table 3) of 13 exhibited six methyl groups at δ_{H} 1.88 (s, 1-OAc), 1.30 (s, Me-10), 1.03 (s, Me-14), 0.99 (s, Me-15), 0.97 (d, Me-20), and 0.95 (d, Me-19) as well as four oxygenated protons at δ_{H} 4.98 (t, H-1), 4.85 (dt, H-13a), 4.50 (ddd, H-13b), and 4.04 (d, H-17). The COSY correlations between H-1/H-2ab/H-3ab, and between H-5/H-6ab/H-7ab together with the HMBC correlations from Me-10 to C-1, C-5, C-8 and C-9, from Me-14 to C-3, C-4, C-5 and C-15, from H-7ab to C-8 and C-11, and from H-13ab to C-8, C-11 and C-12 established a bicyclic sesquiterpene skeleton (from C-1 to C-15) as shown (Fig. 2). In addition, the HMBC correlations from the protons of the methyl at δ_{H} 1.88 and H-1 to the carbonyl carbon at δ_{C} 173.4 indicated the location of an acetoxy group at C-1. The remaining signals suggested the presence of a valine moiety, which was confirmed by the COSY correlations between H-17/H-18/Me-19(20) and the HMBC correlations from H-17 and H-18 to C-16. The above substructures accounted for six degrees of unsaturation, suggesting the presence of an additional ring. In the HMBC spectrum, H-13ab showed correlations to C-16 while H-17 showed a correlation to C-12, indicating the linkage between the sesquiterpene moiety and the valine moiety through ester and amide bonds to form the third seven-membered ring. The relative configuration of the sesquiterpene part was assigned by coupling constants and NOE relationships. The large value of $^2J_{\text{H-2a/H-3a}}$ (13.8 Hz) and the small values of $^2J_{\text{H-1/H-2a}}$ and $^2J_{\text{H-1/H-2b}}$ (both 2.6 Hz) suggested *trans* diaxial orientation of H-2a (δ_{H} 2.07) and H-3a (δ_{H} 1.60) and equatorial orientation of H-1. Assuming that H-1 was on the β -face of the cyclohexane ring, H-2a and H-3b (δ_{H} 1.35) are suggested to be on the β -face of the ring whereas H-2b (δ_{H} 1.78) and H-3a are orientated on the α -face. The ROESY correlations from Me-10 to H-1, H-2a and Me-15 placed Me-10 on the β -face of the ring whereas the ROESY correlations from H-5 to H-3a and Me-14 placed H-5 on the α -face of the ring. After acid hydrolysis of 13 followed by Marfey's reaction, the valine moiety was determined to have L absolute configuration (17S).

In order to elucidate the absolute configuration of the other chirality centers in 13, the solution TDDFT-ECD method was applied on the (1*S*,5*S*,9*S*,17*S*) and (1*R*,5*R*,9*R*,17*S*) stereoisomers.^{21,22} The Merck Molecular Force Field (MMFF) conformational search resulted in 16 and 11 conformers in a 21 kJ mol^{−1}



Table 2 ^1H and ^{13}C NMR data of compound **2** and **3**

Position	2^a		3^b	
	δ_{C} , type	δ_{H} (J in Hz)	δ_{C} , type	δ_{H} (J in Hz)
1	58.1, CH ₂	4.41, d (15.6) 4.01, d (15.6)	57.0, CH ₂	4.55, d (15.8) 4.07, d (15.8)
2	127.7, C		126.9, C	
3	200.0, C		197.4, C	
4	77.2, C		74.1, C	
5	75.0, CH	3.98, t (3.5)	74.7, CH	5.29, dd (3.6, 2.3)
6	37.3, CH ₂	2.70, dd (18.8, 3.5) 2.44, dd (18.8, 3.5)	34.3, CH ₂	2.74, dd (19.5, 3.6) 2.47, dd (19.5, 2.3)
7	149.2, C		147.2, C	
8	41.8, CH ₂	2.35, d (18.9) 2.11, d (18.9)	40.8, CH ₂	2.30, d (18.9) 2.10, d (18.9)
9	96.4, C		94.9, C	
10	34.9, CH ₂	1.69, m 1.54, m	33.8, CH ₂	1.70, m 1.51, m
11	20.0, CH ₂	1.92, m 1.62, m	18.9, CH ₂	1.92, m 1.63, m
12	33.4, CH ₂	1.62, m 1.20, m	32.2, CH ₂	1.61, m 1.19, m
13	68.2, CH	3.80, m	66.9, CH	3.77, m
14	22.0, CH ₃	1.08, d (6.3)	21.7, CH ₃	1.09, d (6.4)
15	22.7, CH ₃	1.30, s	23.7, CH ₃	1.40, s
5-OAc			170.5, C	
			21.1, CH ₃	2.01, s

^a Measured in CD₃OD (^1H at 600 MHz and ^{13}C at 150 MHz). ^b Measured in CDCl₃ (^1H at 600 MHz and ^{13}C at 150 MHz).

Table 3 ^1H and ^{13}C NMR data of compound **13**^a

Position	δ_{C} , type ^b	δ_{H} (J in Hz)
1	75.9, CH	4.98, t (2.6)
2	23.1, CH ₂	2.07, dddd (15.2, 13.8, 4.2, 2.6) 1.78, dddd (15.2, 4.3, 2.6, 2.6)
3	36.2, CH ₂	1.60, ddd (13.8, 13.8, 4.3) 1.35, ddd (13.8, 4.2, 2.6)
4	33.7, C	
5	46.6, CH	1.85, dd (12.6, 1.8)
6	18.8, CH ₂	1.97, m 1.66, m
7	22.5, CH ₂	2.35, m 2.11, m
8	170.3, C	
9	42.3, C	
10	21.3, CH ₃	1.30, s
11	126.3, C	
12	172.4, C	
13	69.9, CH ₂	4.85, dt (17.2, 2.8) 4.50, ddd (17.2, 3.6, 1.3)
14	33.6, CH ₃	1.03, s
15	21.8, CH ₃	0.99, s
16	171.7, C	
17	61.1, CH	4.04, d (7.1)
18	31.0, CH	2.02, m
19	19.5, CH ₃	0.95, d (6.8)
20	19.1, CH ₃	0.97, d (6.8)
1-OAc	173.4, C	
	22.0, CH ₃	1.88, s

^a Measured in CD₃OD (^1H at 600 MHz and ^{13}C at 150 MHz). ^b Data were extracted from the HSQC and HMBC spectra.

energy window, respectively, which were reoptimized separately at the B3LYP/6-31+G(d,p), the ω B97X/TZVP^{23,24} PCM/MeCN, the CAM-B3LYP/TZVP²⁵ PCM/MeCN and the SOGGA11-X/TZVP^{24,26} SMD/MeCN levels of theory. Interestingly, Boltzmann-averaged ECD spectra of both diastereomers computed for conformers over 1% Boltzmann-population at various levels of theory gave moderate to good mirror-image agreement with the experimental ECD spectrum of **13** indicating that the seven-membered ring with C-17 chirality center has the major contribution to the ECD spectrum²² and suggested (1*R*) absolute configuration, opposite to that of the Marfey's analysis. However, while almost all low-energy conformers of (1*S*,5*S*,9*S*,17*S*)-**13** gave similarly mirror-image spectra to the experimental one, for (1*R*,5*R*,9*R*,17*S*)-**13** even highly populated conformers (and the lowest-energy ω B97X/TZVP PCM/MeCN one) gave moderate agreement with the measured ECD and the ratio of the Boltzmann-weights of conformers with congruent and mirror-image spectra is comparable at all applied levels of theory. Although some of the best performing DFT functionals were utilized as suggested by Bremond *et al.* in a recent study,²⁴ no combination of methods could be found, which would suggest the (1*R*,5*R*,9*R*,17*S*)-**13** absolute configuration. With the result of Marfey's analysis in hand, this demonstrated that the small difference in the two ensembles of conformers, having opposite ECD spectra, could not be predicted properly, which is the reason of the failure. Specific optical rotation (SOR) calculations were also performed for the CAM-B3LYP/TZVP PCM/MeOH conformers but resulting in



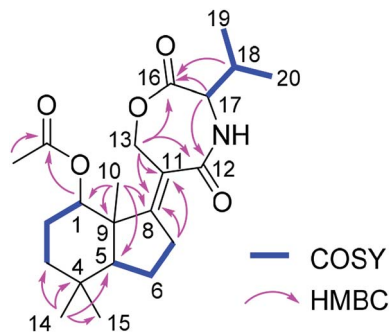


Fig. 2 COSY and key HMBC correlations of **13**.

similarly large negative average values with both levo- and dextrorotating low-energy conformers for both stereoisomers, which did not allow a solid assignment of the absolute configuration. The limited amount of **13** did not allow a VCD measurement. Thus, based on the Marfey's reaction and the ECD results, the structure of **13** was tentatively elucidated as shown, for which a trivial name humigriseamide is proposed.

Asteriquinone CT4 (**14**) is a dimeric tryptophan derivative. In rice approximately 8% of the dry weight consists of proteins whereas the tryptophan content amounts to approximately 1.7% of the total amino acid content.²⁷ Since peas are much richer in proteins compared to rice (20% vs. 8% of the dry weight), we assumed that a higher tryptophan content in peas might be responsible for the formation of **14** during the OSMAC experiment. To test this hypothesis, we added 2% tryptophan to the rice media in order to simulate an excess of tryptophan which resulted in the formation of compound **14** together with another new compound **15** and the known compounds anthranilic acid and *N*-formyl anthranilic acid.

Compound **15** has the molecular formula $C_{21}H_{25}NO_8$ as deduced from the HRESIMS data, corresponding to ten degrees of unsaturation. The 1H and ^{13}C NMR data of **15** (Table 4) were similar to those of the co-isolated bismacrolactone colletotketol (**11**)^{18–20} except for the disappearance of signals of the isolated double bond (C-12/C-13) and the presence of additional signals of one methine group (δ_C 49.8 and δ_H 4.57, CH-13), one methylene group (δ_C 41.8 and δ_H 3.16, 2.95, CH_2 -12) and of four aromatic protons at δ_H 7.81 (H-21), 7.38 (H-19), 6.69 (H-18) and 6.64 (H-20) in **15**. An anthranilic acid moiety was established by the COSY correlations between H-18/H-19/H-20/H-21 and the HMBC correlations from H-19 to C-17 (δ_C 149.2) and from H-21 to C-17 and C-23 (δ_C 169.7) taking also into account the molecular formula of **15**. In addition, the COSY correlations between H_{ab} -12/H-13/13-NH along with the HMBC correlations from H-12ab to C-11 (δ_C 209.1) and C-14 (δ_C 172.3), from H-13 to C-11, C-14 and C-17, and from 13-NH to C-14 indicated the attachment of the anthranilic acid moiety at C-13 through an amide bond. Detailed analysis of the 2D NMR spectra of **15** revealed that the remaining substructure of **15** was identical to that of colletotketol (**11**). Thus, compound **15** was identified as 13-*N*-(2-carboxyphenyl)colletotketol. Based on the biogenetic relationship and similarity of coupling constants and NOE correlations between **11** and **15**, the stereochemistry at C-2, C-8

Table 4 1H and ^{13}C NMR data of compound **15**^a

Position	δ_C , type	δ_H (J in Hz)
2	71.2, CH	4.68, ddq (11.9, 2.7, 6.1)
3	37.1, CH_2	2.49, ddd (11.9, 8.0, 2.7) 2.33, td (11.9, 8.0)
4	143.6, CH	6.67, dt (15.8, 8.0)
5	125.1, CH	5.77, d (15.8)
6	164.5, C	
8	65.2, CH	5.08, ddq (11.3, 1.9, 6.3)
9	38.4, CH_2	2.17, dd (14.2, 11.2) 1.96, ddd (14.2, 7.5, 1.9)
10	73.0, CH	4.03, d (7.5)
11	209.1, C	
12	41.8, CH_2	3.16, dd (18.8, 6.0) 2.95, dd (18.8, 2.0)
13	49.8, CH	4.57, ddd (7.1, 6.0, 2.0)
14	172.3, C	
15	20.0, CH_3	1.17, d (6.3)
16	20.5, CH_3	1.29, d (6.1)
17	149.2, C	
18	111.4, CH	6.69, br d (7.9)
19	134.5, CH	7.38, td (7.9, 1.6)
20	115.5, CH	6.64, br t (7.9)
21	131.9, CH	7.81, dd (7.9, 1.6)
22	111.2, C	
23	169.7, C	
13-NH		8.13, d (7.1)

^a Measured in DMSO- d_6 (1H at 600 MHz and ^{13}C at 150 MHz).

and C-10 in **15** was suggested to be identical to that in **11**, where the absolute configuration had been determined by X-ray analysis.¹⁹ In order to confirm this and determine the absolute configuration of the additional C-13 chirality center, the experimental ECD, VCD, ^{13}C NMR chemical shifts and characteristic $^3J_{H,H}$ coupling constants were calculated for the stereoisomers (2*R*,8*R*,10*R*,13*R*)-**15** and (2*R*,8*R*,10*R*,13*S*)-**15**.²⁸

The MMFF conformational search of (2*R*,8*R*,10*R*,13*R*)-**15** and (2*R*,8*R*,10*R*,13*S*)-**15** resulted in 197 and 246 conformers, respectively, which were reoptimized at the B3LYP/6-31+G(d,p), the B3LYP/TZVP PCM/CHCl₃, the ω B97X/TZVP PCM/MeCN and the mPW1PW91/6-311+(2d,p) SMD/CHCl₃ levels of theory, separately. ^{13}C NMR shift calculations performed both at the mPW1PW91/6-311+(2d,p) *in vacuo* and the mPW1PW91/6-311+(2d,p) SMD/CHCl₃ levels for the B3LYP/6-31+G(d,p) conformers gave similar results for the two stereoisomers indicating no preference of any of the two diastereomers.^{29,30} The ω B97X/TZVP PCM/MeCN conformers (>1%) of (2*R*,8*R*,10*R*,13*R*)-**15** and (2*R*,8*R*,10*R*,13*S*)-**15** showed different conformations for the macrolactone ring, which was also manifested in the dihedral angles $\omega_{H-13,C-13,C-12,H-12ab}$ and $\omega_{H-13,C-13,NH}$. Thus the coupling constants $^3J_{H-13,NH}$, $^3J_{H-12a,H-13}$ and $^3J_{H-12b,H-13}$ were selected for calculations, for which 7.1, 6.0 and 2.0 Hz values were measured, respectively. The computed coupling constants of (2*R*,8*R*,10*R*,13*R*)-**15** gave consistently better agreement with the experimental values than those of (2*R*,8*R*,10*R*,13*S*)-**15**, which had systematically larger values (Table 5). The largest and decisive difference could be observed for 6.0 Hz $^3J_{H-12a,H-13}$ experimental value, which was calculated 5.5 Hz for (2*R*,8*R*,10*R*,13*R*)-**15** and 11.2 Hz for (2*R*,8*R*,10*R*,13*S*)-



Table 5 Comparison of characteristic experimental and computed [mPW1PW91/6-311+G(2d,p)//B3LYP/6-31+G(d,p)] $^3J_{H,H}$ coupling constants of **15**

	$^3J_{H-13,NH}$	$^3J_{H-12a,H-13}$	$^3J_{H-12b,H-13}$
Experimental	7.1	6.0	2.0
(2 <i>R</i> ,8 <i>R</i> ,10 <i>R</i> ,13 <i>R</i>)- 15	8.6	5.5	2.9
(2 <i>R</i> ,8 <i>R</i> ,10 <i>R</i> ,13 <i>S</i>)- 15	9.2	11.2	4.1

15. H-13 and H-12a had *gauche* orientation in (2*R*,8*R*,10*R*,13*R*)-**15** with small $\omega_{H-13,C-13,C-12,H-12a}$ dihedral angles and coupling constants, while H-13 and H-12a had near *trans-periplanar* arrangement in the computed conformers of (2*R*,8*R*,10*R*,13*S*)-**15**, which gave rise to large coupling constant (11.2 Hz). The computed $^3J_{H,H}$ coupling constants clearly suggested that **15** has (2*R**,8*R**,10*R**,13*R**) relative configuration.

^{13}C NMR shifts were also computed for the mPW1PW91/6-311+(2d,p) SMD/CHCl₃ conformers at the same level and although this level gave worse agreement for both stereoisomers because of the rather limited number of compounds utilized for the NMR parameter generation,³¹ it gave considerably better agreement for (2*R*,8*R*,10*R*,13*R*)-**15** than for (2*R*,8*R*,10*R*,13*S*)-**15** in line with the result of the coupling constant calculations. ECD calculations performed at various levels for the B3LYP/6-31+G(d,p) and the $\omega\text{B97X/TZVP}$ PCM/MeCN conformers gave similarly good agreement for both stereoisomers verifying the (2*R*,8*R*,10*R*) absolute configuration of the three stereocenters but giving no information about the C-10 chirality center (Fig. 3 and 4). However, with the combination of the (2*R**,8*R**,10*R**,13*R**) relative configuration from the coupling constants and (2*R*,8*R*,10*R*) absolute configuration from the ECD calculations allowed determining the (2*R*,8*R*,10*R*,13*R*) absolute configuration for **15**. VCD measurement and calculations were also carried out to check whether it can differentiate between the (2*R*,8*R*,10*R*,13*R*) and (2*R*,8*R*,10*R*,13*S*) stereoisomers independently from other

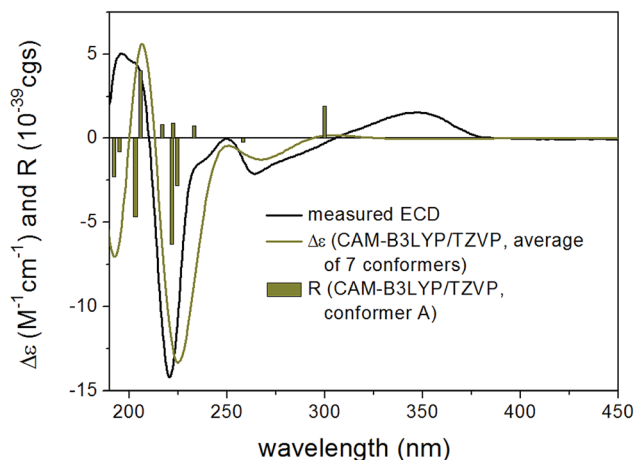


Fig. 4 Experimental ECD spectrum of **15** in MeCN compared with the Boltzmann-weighted CAM-B3LYP/TZVP PCM/MeCN ECD spectrum of (2*R*,8*R*,10*R*,13*S*)-**15**. Level of optimization: $\omega\text{B97X/TZVP}$ PCM/MeCN. Bars represent the rotatory strength values of the lowest-energy conformer.

methods (Fig. 5). VCD calculations performed on the B3LYP/TZVP PCM/CHCl₃ conformers at the same level gave acceptable agreement for both stereoisomers with a slight preference for the (2*R*,8*R*,10*R*,13*R*) stereoisomer. Similarity indexes (ESI†)³² computed with the CDSpecTech package^{33,34} gave considerably higher number (0.335 and a confidence level of 85.4%) for this stereoisomer than for (2*R*,8*R*,10*R*,13*S*)-**15** (0.128). Although this ESI† number is below the limit that Covington and Polavarapu suggested for a safe elucidation of configuration with VCD,³⁴ similarly to the ECD calculations it allowed determining the absolute configuration of **15** as (2*R*,8*R*,10*R*,13*R*) when combined with the result of the coupling constant calculations.

All compounds except for compounds **9** and **14** due to their low amounts were submitted to a cytotoxicity assay using the L5178Y mouse lymphoma cell line and to antimicrobial assay against *Mycobacterium tuberculosis*, *Staphylococcus aureus*,

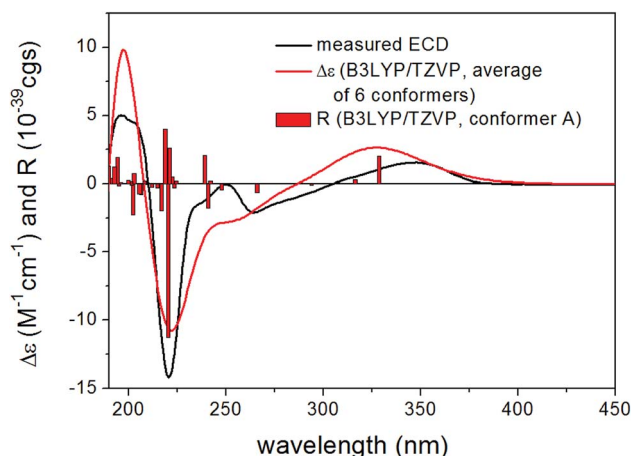


Fig. 3 Experimental ECD spectrum of **15** in MeCN compared with the Boltzmann-weighted B3LYP/TZVP PCM/MeCN ECD spectrum of (2*R*,8*R*,10*R*,13*R*)-**15**. Level of optimization: $\omega\text{B97X/TZVP}$ PCM/MeCN. Bars represent the rotatory strength values of the lowest-energy conformer.

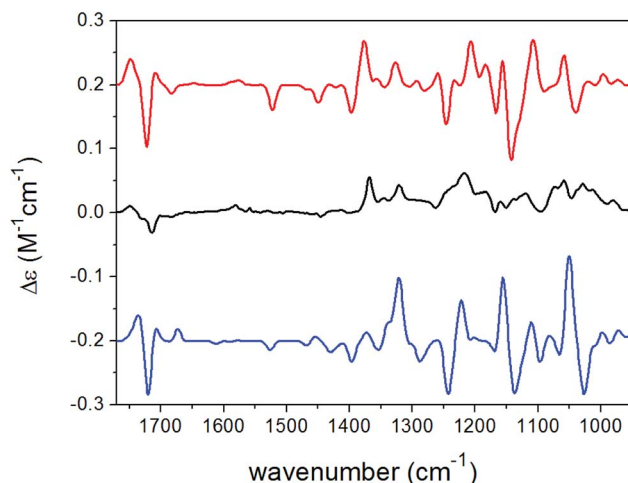


Fig. 5 Experimental VCD spectrum (black line) of **15** in CDCl₃ compared with the Boltzmann-weighted B3LYP/TZVP PCM/CHCl₃ VCD spectra of (2*R*,8*R*,10*R*,13*R*)-**15** (red line) and (2*R*,8*R*,10*R*,13*S*)-**15** (blue line).



Enterococcus faecalis, *Acinetobacter baumannii*, *Pseudomonas aeruginosa* and *Escherichia coli*. Chateochromin A (7), colletotketol (11) and the new compound 15 exhibited strong cytotoxicity with IC₅₀ values of 0.3, 0.5 and 0.2 μM , respectively. Only chateochromin A (7) showed antibacterial activity against *E. faecalis* with an MIC value of 6.3 μM . The remaining compounds were inactive when tested at a dose of 10 μM .

In conclusion, an axenic fermentation of *Trichocladium* sp. on rice medium yielded ten natural products including two new compounds (1 and 3). Co-cultivation of the fungus with *B. subtilis* led to the production of a further new compound (2) and a 10-fold increase of 11. The latter compound is known as a weak broad-spectrum antibiotic,²⁰ implying a possible defense reaction of the fungus against *B. subtilis*. A switch from solid rice to peas as medium for fungal cultivation resulted in the production of an additional new compound 13, representing a sesquiterpene connected with an amino acid. In addition, a dimeric tryptophan derivative 14 was isolated. These results indicate that a protein rich medium such as peas induces the accumulation of different compounds compared to a carbohydrate rich medium like rice. Addition of tryptophan to the rice medium which was done trying to mimic the higher protein content of peas vs. rice caused the accumulation of the new compound 15 which in addition to colletotketol (11) includes anthranilic acid, the latter probably being a fungal biotransformation product of added tryptophan.³⁵

Experimental section

General experimental procedures

Optical rotations were measured on a PerkinElmer-241 MC polarimeter. ECD spectra were recorded on a J-810 spectropolarimeter. VCD measurements were performed on a BioTools ChiralIR-2X spectrometer at a resolution of 4 cm^{-1} under ambient temperature for 18×3000 scans, respectively. Sample was dissolved in CDCl_3 at a concentration of 0.095 M (15), and the solution was placed in a 100 μm BaF_2 cell. NMR spectra were recorded on Bruker ARX 300 or AVANCE DMX 600 NMR spectrometers. Mass spectra were obtained from a Finnigan LCQ Deca XP mass spectrometer while high resolution mass spectra were recorded on a FTHRMS-Orbitrap (Thermo-Finnigan) mass spectrometer. A Dionex P580 system was used in combination with a diode array detector (UVD340S) and an Eurosphere 10 C₁₈ column (125 \times 4 mm) for HPLC analysis and recording UV spectra. Semi-preparative HPLC was conducted on a Lachrom-Merck Hitachi system (pump L7100, UV detector L7400, Eurospher 100 C₁₈ column, 300 \times 8 mm, Knauer Germany). Sephadex-LH20 and Merck MN silica gel 60M (0.04–0.063 mm) were used as stationary phases for column chromatography. TLC plates precoated with silica gel 60 F254 were used for monitoring separation. For spectroscopic measurements spectral grade solvents were used.

Fungal material

Houttuynia cordata was grown in a local garden at Willich, Germany. The identification of the plant used in this study was performed by Dr Marc Appelhans (Department of Systematics,

Biodiversity and Evolution of Plants with Herbarium, Göttingen University). A voucher specimen of the plant (code GOET038305) has been deposited in Göttingen University Herbarium. Fresh roots were harvested in April 2016 and washed with sterilized water, surface sterilized with 70% ethanol for 1 min, and cut into small pieces (around 1 \times 1 \times 1 cm) using a flame sterilized blade. These pieces were put on malt agar plates (15 g L^{-1} malt extract, 15 g L^{-1} agar, and 0.2 g L^{-1} chloramphenicol in distilled water, pH 7.4–7.8 with sodium hydroxide or hydrochloric acid), and then incubated at room temperature for several days. A fungus that was growing out from the root segments was identified as *Trichocladium* sp. using a molecular protocol as described previously.³⁶ Sequence data were submitted to GenBank with the accession number MK241585. A voucher strain (code HCRSW) is kept in the Institute of Pharmaceutical Biology and Biotechnology, Heinrich-Heine University, Düsseldorf, Germany. After surface sterilization we also imprinted the surface sterilized roots on agar plates. Following incubation of these agar plates no fungal growth was detected which proves that the fungus is an endophyte and not an exophyte.

Fermentation and co-cultivation

Fermentation of the fungus was conducted in 11 Erlenmeyer flasks on solid rice medium (100 g rice in 110 mL water followed by autoclaving) at 20 $^\circ\text{C}$ at static conditions. After 33 days each flask was extracted with 600 mL EtOAc. The rice medium was cut into small pieces and shaken for 8 hours followed by evaporation of EtOAc.

Co-cultivation experiment with *Bacillus subtilis* (ATCC168) was conducted on solid rice medium. A total of 15 flasks was prepared (5 axenic fungal cultures as controls, 5 co-cultures with bacteria and 5 axenic bacterial cultures as controls). After addition of 10 mL bacteria solution to each flask, the flasks were incubated at 30 $^\circ\text{C}$ for three days. Then a constant number of pieces from agar plates containing *Trichocladium* sp. were transferred to the co-culture flasks. All flasks were inoculated at 20 $^\circ\text{C}$ under static conditions. After 33 days 600 mL EtOAc was added to each flask in order to terminate the cultivation.

OSMAC experiments

In addition to rice, peas (*Pisum sativum*, from Müllers Mühle, Germany) were used as medium (100 g of peas in 110 mL of H_2O followed by autoclaving). The cultivation procedure was the same as described for cultivation on rice medium. For the feeding experiment using tryptophan, the rice medium was spiked with 2% tryptophan prior to autoclaving.

Extraction and isolation

The crude extract (12 g) obtained from axenic fungal rice cultures was subjected to silica gel vacuum liquid chromatography (VLC) using a step gradient of *n*-hexane/EtOAc and $\text{CH}_2\text{Cl}_2/\text{MeOH}$ to give 11 fractions (V1–V11). Fraction V4 (4.6 g) was further fractionated by reversed phase vacuum liquid chromatography using a step gradient of H_2O and MeOH to yield 10 subfractions (V4RP1–V4RP10). Subfraction V4RP5 was subjected to



a Sephadex LH-20 column using MeOH as eluent followed by purification by semi-preparative HPLC using 55% MeOH–H₂O to give **1** (6.4 mg), **9** (1.2 mg) and **11** (4.5 mg). Following a similar procedure as described for V4RP5, **3** (2.4 mg) and **5** (5.2 mg) were isolated from subfraction V4RP6. Compounds **4** (5.4 mg) and **10** (6.4 mg) were isolated from subfraction V4RP7, while **8** (6.8 mg) was obtained from subfraction V4RP9. Compounds **6** (2.8 mg) and **7** (3.2 mg) were obtained from fractions V6 and V9, respectively, after separation by Sephadex LH-20 column chromatography with MeOH as eluent.

The chromatographic work up of the OSMAC extracts followed the same procedure as described for the axenic rice cultures. Silica gel vacuum liquid chromatography using a step gradient of *n*-hexane/EtOAc and CH₂Cl₂/MeOH was used for separation of the crude extracts obtained from co-cultivation, pea medium and rice medium with addition of tryptophan. A total of ten fractions (CV1–CV10) was obtained from the co-culture extract. Fraction CV4 (2.4 g) was separated by a Sephadex LH-20 column with MeOH as mobile phase followed by purification using semi-preparative HPLC with 45% MeOH–H₂O as eluting system to afford **2** (4.3 mg). The pea culture yielded nine subfractions (PV1–PV9) after VLC. Compounds **12** (6.4 mg) and **13** (5.4 mg) were isolated from fraction PV6, while **14** (0.5 mg) was obtained from fraction PV9 by semi-preparative HPLC using a gradient of MeOH–H₂O (from 10 : 90 to 90 : 10).

Fraction TV6 (854 mg) was obtained from rice medium after addition of tryptophan. The fraction was submitted to silica gel VLC and purified using reversed phase VLC and a step gradient of H₂O and MeOH to give **15** (22.5 mg).

Amidepsine L (1). Pale yellow powder; $[\alpha]_D = +50$ (*c* 0.2, MeOH); UV (MeOH) λ_{\max} 255 and 213 nm; ¹H and ¹³C NMR data see Table 1; HRESIMS *m/z* 620.1370 [M + Na]⁺ (calcd for C₂₉H₂₇NO₁₃Na, 620.1375).

5-Epi-pestafolide A (2). White amorphous solid; $[\alpha]_D = -55$ (*c* 0.05 CH₃OH); UV (MeOH) λ_{\max} 248 nm; ¹H and ¹³C NMR data see Table 2; HRESIMS *m/z* 283.1544 [M + H]⁺ (calcd for C₁₅H₂₃O₅, 283.1540).

5-O-Acetyl-epi-pestafolide A (3). White amorphous solid; $[\alpha]_D = -51$ (*c* 0.05 MeOH); UV (MeOH) λ_{\max} 246 nm; ¹H and ¹³C NMR data see Table 2; HRESIMS *m/z* 325.1651 [M + H]⁺ (calcd for C₁₇H₂₅O₆, 325.1646).

Humigriseamide (13). White amorphous solid; $[\alpha]_D = +34$ (*c* 0.05, MeOH); UV (MeOH) λ_{\max} 216 nm; ECD (MeCN, λ [nm] ($\Delta\epsilon$), *c* 0.128 mM): 289sh (+0.04), 243 (+0.47), 212 (−2.33), 191sh (−2.33); ¹H and ¹³C NMR data see Table 3; HRESIMS *m/z* 392.2433 [M + H]⁺ (calcd for C₂₂H₃₄NO₅, 392.2431).

13-N-(2-Carboxyphenyl)colletoketol (15). Light red oil; $[\alpha]_D = -50$ (*c* 0.05, CHCl₃); UV (MeOH) λ_{\max} 348, 252 and 214 nm; ECD (MeCN, λ [nm] ($\Delta\epsilon$), *c* 0.075 mM): 348 (+1.56), 264 (−2.11), 237sh (−1.41), 220 (−14.20), 203sh (+4.49), 196 (+5.02); ¹H and ¹³C NMR data see Table 4; HRESIMS *m/z* 420.1660 [M + H]⁺ (calc. for C₂₁H₂₆NO₈ 420.1653).

Marfey's analysis

Marfey's analysis was conducted following a previously described protocol.³⁷ Acid hydrolysis of the isolated compounds

1 and **13** was conducted using 0.2 mg of each compound. After addition of 2 mL of 6 N HCl and incubation for 24 h at 110 °C, the acid was removed by drying under a nitrogen stream. 50 μ L of each sample was treated with 100 μ L of FDNPL (1% *N*-(5-fluoro-2,4-dinitrophenyl)-L-leucin amide) in acetone together with 20 μ L 1 M NaHCO₃. Then the mixtures were incubated at 40 °C for 1 h under constant mixing. Next 10 μ L of 2 N HCL was added to each vial followed by evaporation to dryness. For injection to HPLC, 1 mL MeOH was added to each vial. L- and D-amino acids which were used as standards were treated in the same manner. Analysis of the derivatized amino acids was performed by comparing their retention times with those of standards.

Computational methods

Mixed torsional/low-mode conformational searches were carried out by means of the MacroModel 10.8.011 software using the MMFF with an implicit solvent model for CHCl₃ applying a 21 kJ mol^{−1} energy window.³⁸ Geometry reoptimizations of the resultant conformers [B3LYP/6-31+G(d,p) level *in vacuo*, B3LYP/TZVP PCM/CHCl₃, ω B97X/TZVP and CAM-B3LYP/TZVP with PCM solvent model for MeCN, SOGGA11-X/TZVP SMD/MeCN and mPW1PW91/6-311+G(2d,p) SMD/CHCl₃] and DFT VCD, TDDFT ECD and SOR calculations were performed with Gaussian 09 for ECD and SOR using various functionals (B3LYP, BH&HLYP, CAM-B3LYP, PBE0) and the TZVP basis set with the same or no solvent model as in the preceding DFT optimization step.³⁹ ECD spectra were generated as the sum of Gaussians with 3000 cm^{−1} half-height widths, using dipole-velocity-computed rotational strengths.⁴⁰ VCD spectra were calculated with 8 cm^{−1} half-height width and scaled by a factor of 0.98.⁴¹ Boltzmann distributions were estimated from the B3LYP, ω B97X, CAM-B3LYP, SOGGA11-X and mPW1PW91 energies. ESI⁺ values were computed with the CDSpecTech 22.0 software package.^{32–34} The MOLEKEL program was used for visualization of the results.⁴²

Cytotoxicity assay

Cytotoxicity against the L51178Y mouse lymphoma cell line was measured using the MTT assay.⁴³ Kahalalide F and 0.1% ethylene glycol monomethyl ether in DMSO were used as positive and negative control, respectively.

Antimicrobial assay

Antimicrobial activity of the compounds was conducted using the microdilution method. Compounds were dissolved in DMSO and added to the broth. The resulting final DMSO concentration in the assay was 0.1%. The direct colony suspension method was employed for preparation of the inoculum, and MIC values for each strain were determined according to the recommendations of the Clinical and Laboratory Standards.⁴⁴ Two known antibiotics, ciprofloxacin and moxifloxacin (analytical standard, Sigma-Aldrich) were used as positive controls.



Conflicts of interest

There are no conflicts to declare.

Acknowledgements

This project was funded by the Deutsche Forschungsgemeinschaft (project number 270650915, GRK 2158). Further support by the Manchot Foundation to P. P. is gratefully acknowledged. The Hungarian authors were supported by the EU and co-financed by the European Regional Development Fund under the project GINOP-2.3.2-15-2016-00008. T. K. and A. M. thank the National Research, Development and Innovation Office (NKFI K120181 and PD121020). The Governmental Information-Technology Development Agency (KIFÜ) is acknowledged for CPU time. We furthermore wish to thank Dr Marc Appelhans (Department of Systematics, Biodiversity and Evolution of Plants with Herbarium, Göttingen University, Germany) for identification of the plant material.

References

- 1 M. C. Wani, H. L. Taylor, M. E. Wall, P. Coggon and A. T. McPhail, *J. Am. Chem. Soc.*, 1971, **93**, 2325–2327.
- 2 A. Stierle, G. Strobel and D. Stierle, *Science*, 1993, **260**, 214–216.
- 3 A. H. Aly, A. Debbab and P. Proksch, *Pharmazie*, 2013, **68**, 499–505.
- 4 S. Liu, H. Dai, G. Makhoulfi, C. Heering, C. Janiak, R. Hartmann, A. Mándi, T. Kurtán, W. E. Müller, M. U. Kassack, W. Lin, Z. Liu and P. Proksch, *J. Nat. Prod.*, 2016, **79**, 2332–2340.
- 5 H. Wang, H. F. Dai, C. Heering, C. Janiak, W. H. Lin, R. S. Orfali, W. E. G. Müller, Z. Liu and P. Proksch, *RSC Adv.*, 2016, **6**, 81685–81693.
- 6 H. Wang, P. M. Eze, S. P. Höfert, C. Janiak, R. Hartmann, F. B. C. Okoye, C. O. Esimone, R. S. Orfali, H. F. Dai, Z. Liu and P. Proksch, *RSC Adv.*, 2018, **8**, 7863–7872.
- 7 X. W. Wang, F. Y. Yang, M. Meijer, B. Kraak, B. D. Sun, Y. L. Jiang, Y. M. Wu, F. Y. Bai, K. A. Seifert, P. W. Crous, R. A. Samson and J. Houbraken, *Stud. Mycol.*, 2018, **93**, 65–153.
- 8 U. Mocek, L. Schultz, T. Buchan, C. Baek, L. Fretto, J. Nzerem, L. Sehl and U. Sinha, *J. Antibiot.*, 1996, **49**, 854–859.
- 9 D. Laurent, G. Guella, I. Mancini, M. F. Roquebert, F. Farinole and F. Pietra, *Tetrahedron*, 2002, **58**, 9163–9167.
- 10 J. Inokoshi, Y. Takagi, R. Uchida, R. Masuma, S. Omura and H. Tomoda, *J. Antibiot.*, 2010, **63**, 9–16.
- 11 G. Ding, S. Liu, L. Guo, Y. Zhou and Y. Che, *J. Nat. Prod.*, 2008, **71**, 615–618.
- 12 N. Phonkerd, S. Kanokmedhakul, K. Kanokmedhakul, K. Soyong, S. Prabpai and P. Kongsearee, *Tetrahedron*, 2008, **64**, 9636–9645.
- 13 F. X. Yu, Y. Chen, Y. H. Yang and P. J. Zhao, *Phytochem. Lett.*, 2016, **16**, 263–267.
- 14 K. Koyama, S. Natori and Y. Iitaka, *Chem. Pharm. Bull.*, 1987, **35**, 4049–4055.
- 15 K. Koyama and S. Natori, *Chem. Pharm. Bull.*, 1988, **36**, 146–152.
- 16 N. Morooka, S. Nakano, N. Itoi and Y. Ueno, *Agric. Biol. Chem.*, 1990, **54**, 1247–1252.
- 17 J. Elix and L. Lajide, *Aust. J. Chem.*, 1981, **34**, 2005–2011.
- 18 J. MacMillan and T. J. Simpson, *J. Chem. Soc., Perkin Trans. 1*, 1973, 1487–1493.
- 19 U. Höller, A. D. Wright, G. M. König and P. G. Jones, *Acta Crystallogr., Sect. C: Cryst. Struct. Commun.*, 1999, **55**, 1310–1313.
- 20 T. J. Hunter and G. A. O'Doherty, *Org. Lett.*, 2002, **4**, 4447–4450.
- 21 S. Superchi, P. Scafato, M. Gorecki and G. Pescitelli, *Curr. Med. Chem.*, 2018, **25**, 287–320.
- 22 A. Mándi, I. W. Mudianta, T. Kurtán and M. J. Garson, *J. Nat. Prod.*, 2015, **78**, 2051–2056.
- 23 J. D. Chai and M. Head-Gordon, *J. Chem. Phys.*, 2008, **128**, 084106.
- 24 É. Brémond, M. Savarese, N. Q. Su, Á. J. Pérez-Jiménez, X. Xu, J. C. Sancho-García and C. Adamo, *J. Chem. Theory Comput.*, 2016, **12**, 459–465.
- 25 T. Yanai, D. P. Tew and N. C. Handy, *Chem. Phys. Lett.*, 2004, **393**, 51–57.
- 26 R. Peverati and D. G. Truhlar, *J. Chem. Phys.*, 2011, **135**, 191102.
- 27 V. W. Padhye and D. K. Salunkhe, *Cereal Chem.*, 1979, **56**, 389–393.
- 28 A. Mándi and T. Kurtán, *Nat. Prod. Rep.*, 2019, **36**, 889–918.
- 29 M. W. Lodewyk, M. R. Siebert and D. J. Tantillo, *Chem. Rev.*, 2012, **112**, 1839–1862.
- 30 CHESHIRE CCAT, *The Chemical Shift Repository for computed NMR scaling factors*, <http://cheshirenmr.info/index.htm>.
- 31 S. Qiu, E. de Gussem, K. A. Tehrani, S. Sergeyev, P. Bultinck and W. Herrebout, *J. Med. Chem.*, 2013, **56**, 8903–8914.
- 32 E. Debie, E. de Gussem, R. K. Dukor, W. Herrebout, L. A. Nafie and P. Bultinck, *ChemPhysChem*, 2011, **12**, 1542–1549.
- 33 C. L. Covington and P. L. Polavarapu, *CDSpecTech: Computer programs for calculating similarity measures of comparison between experimental and calculated dissymmetry factors and circular intensity differentials, version 22.0*, 2017, <https://sites.google.com/site/cdspectech1/>.
- 34 C. L. Covington and P. L. Polavarapu, *Chirality*, 2017, **29**, 178–192.
- 35 C. K. Wat and G. H. N. Towers, in *Biochemistry of plant phenolics. Recent advances in phytochemistry*, ed. T. Swain, J. B. Harbone and C. F. Van Sumere, Springer, Boston, MA, 1979, vol 12, Metabolism of the aromatic amino acids by fungi, pp. 371–432.
- 36 J. Kjer, A. Debbab, A. H. Aly and P. Proksch, *Nat. Protoc.*, 2010, **5**, 479–490.
- 37 P. Marfey, *Carlsberg Res. Commun.*, 1984, **49**, 591.
- 38 MacroModel, Schrödinger, LLC, 2015, <https://www.schrodinger.com/MacroModel>.



- 39 M. J. Frisch, G. W. Trucks, H. B. Schlegel, G. E. Scuseria, M. A. Robb, J. R. Cheeseman, G. Scalmani, V. Barone, B. Mennucci, G. A. Petersson, H. Nakatsuji, M. Caricato, X. Li, H. P. Hratchian, A. F. Izmaylov, J. Bloino, G. Zheng, J. L. Sonnenberg, M. Hada, M. Ehara, K. Toyota, R. Fukuda, J. Hasegawa, M. Ishida, T. Nakajima, Y. Honda, O. Kitao, H. Nakai, T. Vreven, J. A. Montgomery Jr, J. E. Peralta, F. Ogliaro, M. Bearpark, J. J. Heyd, E. Brothers, K. N. Kudin, V. N. Staroverov, R. Kobayashi, J. Normand, K. Raghavachari, A. Rendell, J. C. Burant, S. S. Iyengar, J. Tomasi, M. Cossi, N. Rega, J. M. Millam, M. Klene, J. E. Knox, J. B. Cross, V. Bakken, C. Adamo, J. Jaramillo, R. Gomperts, R. E. Stratmann, O. Yazyev, A. J. Austin, R. Cammi, C. Pomelli, J. W. Ochterski, R. L. Martin, K. Morokuma, V. G. Zakrzewski, G. A. Voth, P. Salvador, J. J. Dannenberg, S. Dapprich, A. D. Daniels, Ö. Farkas, J. B. Foresman, J. V. Ortiz, J. Cioslowski and D. J. Fox, *Gaussian 09 (Revision E.01)*, Gaussian, Inc., Wallingford, CT, 2013.
- 40 P. J. Stephens and N. Harada, *Chirality*, 2010, **22**, 229–233.
- 41 A. Mándi, M. M. Swamy, T. Taniguchi, M. Anetai and K. Monde, *Chirality*, 2016, **28**, 453–459.
- 42 U. Varetto, *MOLEKEL 5.4*, Swiss National Supercomputing Centre, Manno, Switzerland, 2009.
- 43 M. Ashour, R. Edrada, R. Ebel, V. Wray, W. Watjen, K. Padmakumar, W. E. Muller, W. H. Lin and P. Proksch, *J. Nat. Prod.*, 2006, **69**, 1547–1553.
- 44 CLSI, *Methods for Dilution Antimicrobial Susceptibility Tests for Bacteria That Grow Aerobically*, Approved Standard Ninth ed. CLSI document M07-A9, Clinical and Laboratory Standards Institute, Wayne, PA, 2012.

